

# Study of phosphor $\text{Ba}_2\text{Si}_3\text{O}_8:\text{Eu}^{2+}$ to produce WLED devices with support from $\text{ZnCdSe}/\text{ZnSe}$ quantum dot

Huu Phuc Dang<sup>1</sup>, Bui Van Hien<sup>2</sup>, Nguyen Le Thai<sup>3</sup>

<sup>1</sup>Institute of Applied Technology, Thu Dau Mot University, Binh Duong Province, Vietnam

<sup>2</sup>Faculty of Mechanical-Electrical and Computer Engineering, School of Engineering and Technology, Van Lang University, Ho Chi Minh City, Vietnam

<sup>3</sup>Faculty of Engineering and Technology, Nguyen Tat Thanh University, Ho Chi Minh City, Vietnam

## Article Info

### Article history:

Received Nov 28, 2021

Revised Jul 11, 2022

Accepted Aug 16, 2022

### Keywords:

$\text{Ba}_2\text{Si}_3\text{O}_8:\text{Eu}^{2+}$

Color homogeneity

Luminous flux

Monte carlo theory

White light-emitting diodes

## ABSTRACT

We created the blue-green  $\text{Ba}_2\text{Si}_3\text{O}_8:\text{Eu}^{2+}$  (or BaE) phosphor treated with  $\text{Eu}^{2+}$  using the standard solid-state method with the concentration of Eu as well as heating temperature properly adjusted for the maximum luminescence efficacy. It is possible to excite the said phosphor using near-UV (n-UV) wavelengths and to display its wide emission band, which is the  $5d \Rightarrow 4f$  shift for  $\text{Eu}^{2+}$ , caused by the combination of the Eu activator and the nearby host. We integrated the said phosphor with the n-UV LED to create the pc-LED (short for diodes based on conversion phosphor). For the task of creating the white light-emitting diode (WLED) device that yields significant color rendering index, we combined the orange  $\text{ZnCdSe}/\text{ZnSe}$  quantum dot with a distinctive sheet structure for the pc-LED made with phosphor BaE. This research demonstrates the electroluminescence features of the said elements.

This is an open access article under the [CC BY-SA](https://creativecommons.org/licenses/by-sa/4.0/) license.



## Corresponding Author:

Bui Van Hien

Faculty of Mechanical-Electrical and Computer Engineering, School of Engineering and Technology

Van Lang University

Ho Chi Minh City, Vietnam

Email: hien.bv@vlu.edu.vn

## 1. INTRODUCTION

Over the time, the white light-emitting diode (WLED) devices went through considerable development, primarily used for optical exhibition. The pc-LED devices are commonly used to create white illumination due to their price being more reasonable than the combined LEDs with colors red, blue and green [1]-[3]. Judging the preferred excitation wavelength for the phosphor, we can employ the InGaN chip based on blue with wavelength range from 440 nm to 460 nm or n-UV with wavelength range from 350 nm to 420 nm to create the pc-LED devices [4], [5]. To easily create a pc-LED device with the lowest cost, we can use a mixture of the LED emits blue light and phosphors emit yellow light like  $\text{Y}_3\text{Al}_5\text{O}_{12}:\text{Ce}^{3+}$  or  $\text{Sr}_3\text{Si}_3\text{O}_8:\text{Ce}^{3+},\text{Li}^{3+}$ . On the other hand, a common flaw of the blue-integrated white LED devices is the low observable range of spectrum with a notable lack of the red element, which results in particularly low certainty of response index (CRI) or  $R_a$  (short for color rendering index). With an n-UV LED, it is possible to daub at least two phosphors to create the pc-LED device. Because of the benefits of the n-UV LED which includes great performance, reliability as well as the lack of its illumination's influence on the chromatic output, the pc-LED devices made of n-UV LED are considered a potential optical generator [6]-[9]. By utilizing the suitable phosphors for the pc-LED devices, it is possible to create various emission colors, which creates high-CRI white illumination as a result. Because of the potent reaction between the  $\text{Eu}^{2+}$  activator and the nearby host lattices, the ions of  $\text{Eu}^{2+}$  with the suitable optical  $5d-4f$  shift displays a band emission as well

as creates various emission wavelengths acting like a function for the selected hosts due to the extent of Stokes transfer for the emission of  $\text{Eu}^{2+}$  being related to the crystal field region as well as the host's covalence impact on the activator. Silicate phosphors treated with  $\text{Eu}^{2+}$  have attracted considerable research interest in cold-light substances and appears to be highly effective phosphors for LEDs because of the unity between the excitation wavelengths of the phosphors and blue or n-UV illuminations. While various stoichiometric host compounds of the said phosphors may exist, the alkaline-earth hosts appear to be the ones most focused on. These hosts are selected to be treated with  $\text{Eu}^{2+}$  such as  $\text{M}_3\text{SiO}_5$ ,  $\text{M}_2\text{SiO}_4$ ,  $\text{M}_2\text{MgSi}_2\text{O}_7$ , and  $\text{M}_3\text{MgSi}_2\text{O}_8$ , [10]-[12]. Certain new researches have synthesized BaE phosphor utilizing the sol gel and analyzed its photoluminescence features. On the other hand, the creation of LEDs has not utilized such phosphor.

Thanks to the innovations of the fabrication techniques for the quantum dots (abbreviated as QDs), many have pointed out their potential benefits for the biological as well as the optoelectronic areas, having effective fluorescence features like significant quantum yield (or QY) and optical reliability. Among the functions of the quantum dots (QDs), there is one involving the QDs to be used in the form of luminescent down-transmuters for the LEDs with the task of absorbing the photon power from the blue or n-UV wavelength of the LED chip as well as generating a distinctive wavelength, which is adjustable via the manipulation of the QDs' proportion as well as constituents [13], [14]. To create LEDs made of QDs, the QDs made of CdSe are usually selected for the easily-adjustable nature in the observable emission on the basis of the blue or n-UV LEDs. Zhang *et al.* [15] utilized the red-light CdSe QDs in the form of a supporting chromatic center for the purpose of raising the CRI for the WLED devices made of the yellow phosphor  $\text{Sr}_3\text{SiO}_5:\text{Ce}^{3+},\text{Li}^+$  due to the devices' lack of red spectrum. For our research, we created the phosphor BaE as well as the ZnCdSe/ZnSe QD using the solid-state method as well as hot solution phase chemistry. In order to properly utilize the phosphor and QD for creating the WLED device, we combined them with an n-UV LED having a distinctive sheet structure, comprising of QD and phosphor sheets as well as examined the electroluminescent features of the phosphor and QD.

## 2. EXPERIMENTAL

### 2.1. Creating the phosphors BaE

We created the phosphors through the standard solid-state technique using the substances which include pure  $\text{BaCO}_3$ ,  $\text{SiO}_2$  as well as  $\text{Eu}_2\text{O}_3$  (99.9%, Kojundo Chem). We predetermined the substances' proportions and combined them with ethanol then let the powders dry under the temperature of  $100^\circ\text{C}$  in an oven. For the phosphor  $\text{Ba}_{2-x}\text{Si}_3\text{O}_8:\text{Eu}_x$ , the concentration  $x$  of Eu fluctuated from 0.005 to 0.07. We pulverized the acquired substance then heated it under the temperature of  $1100^\circ\text{C}$  to  $1300^\circ\text{C}$  for four hours at lowering atmosphere, which is made of 25%  $\text{H}_2$  and 75%  $\text{N}_2$  with a tube furnace. The emission intensity of photoluminescence for the phosphors went up as the heating temperature increased to  $1300^\circ\text{C}$  maximumly. As the temperature exceeds the said threshold, the phosphors took a glass-like form. We heated every phosphor under the temperature of  $1300^\circ\text{C}$  [15], [16].

### 2.2. Creating the WLED devices

With the blue-green phosphor BaE, we created the pc-LED device through daubing the InGaN n-UV LED device positioned on the exterior under the wavelength of  $405 \pm 5$  nm with a blend containing the phosphor and silicone resin (Dow Corning, OE 6630B). We created the orange QD through daubing the said LED with a chlorobenzene mixture containing QD and poly (methyl methacrylate) (PMMA,  $M_w = 120000$ ). We determined the mass proportion between polymethyl methacrylate (PMMA) and QD to be 68-70 and the PMMA concentration of chlorobenzene to be 1.7 mM. To create a WLED device that yields significant CRI, we integrated the phosphor and QD with a chip having the following sheet layout. Initially, we loaded the nUV-LED's mold with a blend containing QD and PMMA then let it dry under the temperature of  $60^\circ\text{C}$  for half an hour for the chlorobenzene to vaporize. The hardened blend of QD and PMMA accounted for roughly under one-fifth of the mold's capacity. We subsequently daubed the blend of phosphor and silicone resin above the QD-PMMA blend then cured it under the temperature of  $70^\circ\text{C}$  for twelve hours, which filled the mold's unused capacity. We took into account a different sheet layout containing the phosphor-resin blend followed by the QD-PMMA blend. However, this layout didn't work as expected due to the chlorobenzene of the QD-PMMA mixture ruined the cured silicone resin.

## 3. RESULTS AND ANALYSIS

In addition to the many impurity-doped semiconductors discussed previously, in which the radiation is driven by electronic transferences inside the impurity ion, semiconductor nanoparticles (or quantum dots, QDs) are suggested as hue transformation substance in LEDs. Quantum confinement may happen with a discretization

of the electronic range configuration if they grow exceedingly small (with a dimension of a few nm). When comparing the bulk case, the band gap energy goes up considerably, owing to the presence of large absorbing highest points because of the discretized power levels [17]-[19].

With the aim to promote effective luminescence, non-radiative degradation through outside covering defect states have to be declined, which may be performed by passivating the organic capping outside covering or by utilizing an inorganic shell. CdSe is put to shame the most often used quantum dot in conjunction with blue pumping LEDs owing to its fairly great quantum effectiveness and adjustability of radiation over the whole visible region. The radiation is quite limited with quantum dot solutions and a constrained dimension dispensation, with an FWHM of roughly 30 nm. This, regarding to the modest Stokes shift, permits the pairing of a blue pumping LED with green and red generating QDs with no leaking a lot of emitting power into the intense-red section of the bands of color, where eye sensitivity is negligible. Jeon *et al.* [19] demonstrated a 41 lm/W effective gadget for flat panel display backlighting according to multi-shelled CdSe-based QDs which emit green and red illumination. Lastly, their small size decreases dispersion losing (compared to traditional phosphors) and enables them to be implanted in transparent matrices. However, the popular usage modern QDs as hue changers is hampered by a number of problems: (i) Cd-based compounds are harmful to the environment, and the amount of substitute, greener hosts with elevated quantum effectiveness, which is required for transformation-based LEDs, is restricted. (ii) When QDs are utilized for green and red radiation, the modest Stokes shift causes significant reabsorption [20]-[22]. To reduce some of the reabsorption, distinct ways of QDs has been considered. (iii) Heat quenching is typically highly strong as comparing to bulk impurity-doped semiconductors, requiring a distant technique for elevated flux gadgets. The illumination from a 450 nm pump LED has been shown to degrade the YAG:Ce nanoparticles organic capping film.

Particles having dimensions range from a few tens of nanometers to hundreds of nanometers are neither QDs nor bulk materials. They are not 'actual' quantum organizations with considerable quantum confinement. These particle sizes, however, are appealing used in clear, refractive index-matched matrices to decrease dispersion losses. The downsides of very tiny particle sizes include a significantly increased surface-to-volume proportion, which increases the effect of non-radiative decomposition paths happened by surface defects. This has the potential to have a negative influence on quantum effectiveness and heat quenching behavior. Dopant incorporation may also be more challenging for littler particles. The wide excitation band increasing to 420 nm maximumly is caused by the shift from the 4f-ground to the 5d-stimulated condition for the ion of  $\text{Eu}^{2+}$ , which means that the phosphor can be utilized for the creation of pc-LED device based on the n-UV LED. The blue-green emission with maximum wavelength of 506 nm and a wide bandwidth of the 5d  $\Rightarrow$  4f shift (from the lowest relaxed 5d state to the  $^8\text{S}_{7/2}$  state) in the ion of  $\text{Eu}^{2+}$ , caused by the potent reaction between 5d electron and the nearby hosts. When it comes to creating white light that yields significant chromatic output, it is better to select a broad band emission. We determined the phosphor's full width at half-maximum as 105 nm, thinner compared to the common yellow phosphor  $\text{Y}_3\text{Al}_5\text{O}_{12}:\text{Ce}$ . The intensity of emission went up as the said concentration raised to 0.05 and went down at 0.07 because of the abatement in concentration, the non-radioactive energy shift among the ions of  $\text{Eu}^{2+}$  via the galvanic multipole-multipole interactivity. Such event was seen earlier for the phosphors treated with  $\text{Ce}^{3+}$  or  $\text{Eu}^{2+}$ . When the concentration of  $\text{Eu}^{2+}$  goes up, the ions of  $\text{Eu}^{2+}$  having greater 5d states are more likely to relax or perform energy shift for the purpose of decreasing the 5d states within the identical or the surrounding  $\text{Eu}^{2+}$  locations, which causes a red emission. The concentrations of BaE green phosphor and YAG: $\text{Ce}^{3+}$  yellow phosphor shown in Figure 1 are in inverse proportion. In other words, the growth green phosphor doping amount results in the decline in yellow phosphor one. Particularly, BaE amount increasing from 2% to 10 % causes YAG: $\text{Ce}^{3+}$  concentration to notably decline. This occurrence is to keep the consistent CCT during the operation and examination and modify the scattering and absorption features of the remote-phosphor configuration. Consequently, it is possible to manage the color and luminous performances by the regulate the integrating concentration of BaE, which is applicable for WLEDs having 5600-8500 K.

Figure 2 presents the emission power of white light from the WLED using remote-phosphor layout with BaE green phosphor. Obviously, the emission power exhibits two notable spectral intensities within the blue and yellow-green wavelengths regions, 420-480 nm and 500-570nm, respectively. These two wavelength regions are imperative for generating white light. The addition of BaE phosphor results in the more intense power with these regions, suggesting the increasing brightness of the WLED light. Besides, the increase in blue illumination wavelength suggests higher activity of the scattering in the phosphor layer and in WLED, which improves chromatic uniformity as a consequence. The data illustrated in Figure 3 also contributes to affirming the effectiveness in using BaE phosphor to elevate the luminous strength of the WLED. As the increasing doping concentration of BaE green phosphor (2% wt to 20% wt.) is introduced to the remote phosphor sheet, the luminous intensities increase substantially. Moreover, as depicted in Figure 4, the color variation of WLED declined with the higher BaE concentration. Such a result may be critical for the BaE application, meaning that the enhanced scattering property with BaE phosphor is efficient. Such results

are crucial to the application of BaE in WLED production, especially to perform the high-CCT WLED with significant color uniformity.

The improvement in color homogeneity with the higher doping concentration of BaE can be attributed to the absorbing activities in a layer of green-emission phosphor. The phosphor particles will absorb the blue-emitted light rays from the blue-LED chip, converts and releases the green light rays eventually. Though the yellow light from the YAG:Ce<sup>3+</sup> also goes through the same mechanism, the its amount is less than the blue one owing to the absorption of characteristic of the green-phosphor spheres. As a result, when BaE is integrated into the remote phosphor sheet, the converted green elements is added, increasing the total proportion of green light in the WLED package, leading to increasing color homogeneity. Color uniformity is an imperative factor for quality white light, hindering that the price of WLED will be more significant if it possesses great color uniformity index. The application of phosphor-converted material could help to elevate the cost-effectiveness, meaning the that using green-emission phosphor BaE can have economic benefits and while be able to attain high-quality WLED products. The manufacturers can easily choose the suitable amount of BaE to use, based on their production goal. When they aim to produced WLED lamps with high color recreation performance, it is acceptable to reduce luminosity slightly.

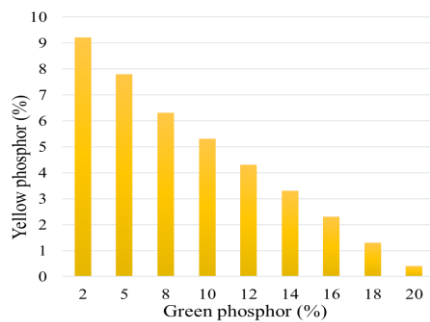


Figure 1. Maintaining the median CCT by altering the phosphor concentration

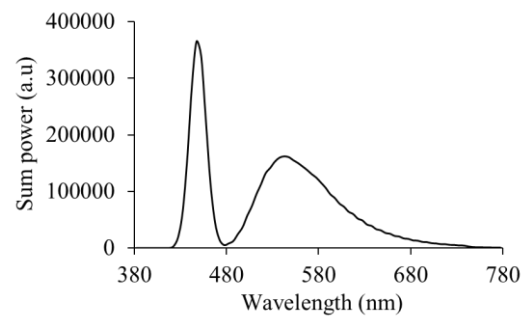


Figure 2. Emission power of white light at 8000 K as a function of BaE utilization

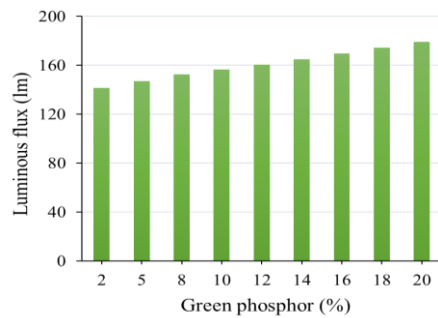


Figure 3. Luminosity of the WLED with different BaE concentrations

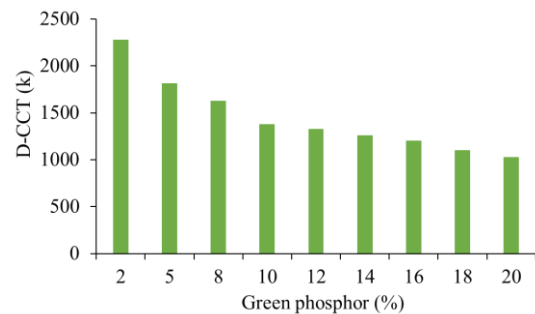


Figure 4. Color variations in the WLED with different BaE concentrations

When defining the hue effectiveness of a certain WLED, we need more than only good color homogeneity. For this reason, the color rendering index and color quality scale, shortened as CRI and cultural intelligence scale (CQS), respectively, are introduced. These indices are utilized for accessing the color rendition of the tested white light. The CRI, particularly, accesses the ability to re-create colors of an object that is lightened by the examined white light. If the white light is insufficient in one or more emission colors of green, blue, yellow, and red, the chromatic homogeneity is diminished. When using BaE green phosphor, the increasing concentration would lead to significant amount of green light to be generated, which can be overabundant, resulting in the shortage in other emission colors. Consequently, the color uniformity is degraded.

The CRI and CQS data of the WLED when using BaE phosphor are described in Figure 5 and Figure 6, respectively. The CRI is lower alongside the increasing concentration of BaE. Meanwhile, the CQS initially increases with the rise of BaE concentration and then declines when this phosphor's concentration is more than

10%wt. Such decreases can be ascribed to the abundant green light demonstrated above. Here, we can tell that the color rendition of the white light is improved with the BaE concentration below 10%wt. as with that concentration limitation, the CQS shows its increase though the CRI decreases. As the CQS is the parameter that covers the CRI, the color coordinate, and the viewer's inclination, it is more beneficial to attain high CQS than obtaining high CRI [23]-[26]. Hence, the concentration of green phosphor BaE must be selected carefully.

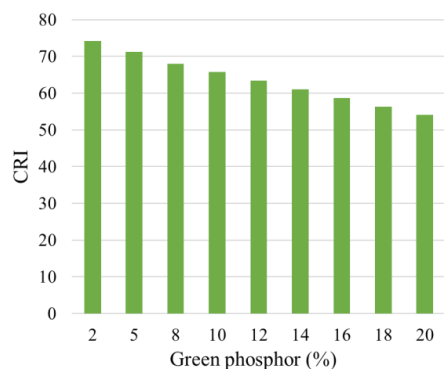


Figure 5. CRI of the WLED with different BaE concentrations

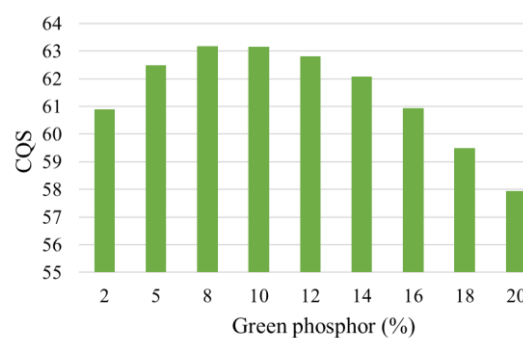


Figure 6. CQS of the WLED with different BaE concentrations

#### 4. CONCLUSION

This work used green-phosphor  $Ba_2Si_3O_8:Eu^{2+}$  to improve the efficiency of the WLED's remote phosphor layout. The phosphor was prepared with the solid-state method; and its luminescent features were analyzed. When using BaE phosphor, the WLED showed notable spectral intensities in blue and yellow-green wavelength areas, denoting the changes in scattering and absorption activities of the phosphor package. The luminosity was improved and the enhancement in color uniformity was attained with the increasing BaE concentration. The color rendition also increased with ~10%wt. BaE doped, as the CQS values showed apparent enhancement. However, the CRI and CQS were reduced if the BaE concentration was more than 10%wt., due to the redundant green light. Therefore, the concentration of BaE must be chosen properly to achieve the desired outcomes.

#### ACKNOWLEDGEMENTS

This study was financially supported by Van Lang University, Vietnam.




#### REFERENCES

- [1] W. J. Kim, T. K. Kim, S. H. Kim, S. B. Yoon, H.-H. Jeong, J.-O. Song, and T.-Y. Seong, "Improved angular color uniformity and hydrothermal reliability of phosphor-converted white light-emitting diodes by using phosphor sedimentation," *Optics Express*, vol. 26, no. 22, pp. 28634-28640, 2018, doi: 10.1364/OE.26.028634.
- [2] Y. Xie *et al.*, "Encapsulated room-temperature synthesized CsPbX<sub>3</sub> perovskite quantum dots with high stability and wide color gamut for display," *Optical Materials Express*, vol. 8, no. 11, pp. 3494-3505, 2018, doi: 10.1364/OME.8.003494.
- [3] M. A. Juratli *et al.*, "Noninvasive label-free detection of circulating white and red blood clots in deep vessels with a focused photoacoustic probe," *Biomed. Optics Express*, vol. 9, no. 11, pp. 5667-5677, 2018, doi: 10.1364/BOE.9.005667.
- [4] D. Molter, M. Kolano, and G. Freymann, "Terahertz cross-correlation spectroscopy driven by incoherent light from a superluminescent diode," *Optics Express*, vol. 27, no. 9, pp. 12659-12665, 2019, doi: 10.1364/OE.27.012659.
- [5] A. Ali. *et al.*, "Blue-laser-diode-based high CRI lighting and high-speed visible light communication using narrowband green-/red-emitting composite phosphor film," *Applied Optics*, vol. 59, no. 17, pp. 5197-5204, 2020, doi: 10.1364/AO.392340.
- [6] S. Beldi *et al.*, "High Q-factor near infrared and visible Al<sub>2</sub>O<sub>3</sub>-based parallel-plate capacitor kinetic inductance detectors," *Optics Express*, vol. 27, no. 9, pp. 13319-13328, 2019, doi: 10.1364/OE.27.013319.
- [7] C. H. Lin *et al.*, "Hybrid-type white LEDs based on inorganic halide perovskite QDs: candidates for wide color gamut display backlights," *Photonics Research*, vol. 7, no. 5, pp. 579-585, 2019, doi: 10.1364/PRJ.7.000579.
- [8] W. Y. Chang, Y. Kuo, Y. W. Kiang, and C. C. Yang, "Simulation study on light color conversion enhancement through surface plasmon coupling," *Optics Express*, vol. 27, no. 12, pp. A629-A642, 2019, 10.1364/OE.27.00A629.
- [9] X. Xi *et al.*, "Chip-level Ce:GdYAG ceramic phosphors with excellent chromaticity parameters for high-brightness white LED device," *Optics Express*, vol. 29, no. 8, pp. 11938-11946, 2021, doi: 10.1364/OE.416486.
- [10] L. Xiao, C. Zhang, P. Zhong, and G. He, "Spectral optimization of phosphor-coated white LED for road lighting based on the mesopic limited luminous efficacy and IES color fidelity index," *Applied Optics*, vol. 57, no. 4, pp. 931-936, 2018, doi: 10.1364/AO.57.000931.
- [11] H. Huang, M. Wei, and L. C. Ou, "White appearance of a tablet display under different ambient lighting conditions," *Optics Express*, vol. 26, no. 4, pp. 5018-5030, 2018, doi: 10.1364/OE.26.005018.




- [12] L. Duan and Z. Lei, "Wide color gamut display with white and emerald backlighting," *Applied Optics*, vol. 57, no. 6, pp. 1338-1344, 2018, doi: 10.1364/AO.57.001338.
- [13] W. Wang and P. Zhu, "Red photoluminescent Eu<sup>3+</sup>-doped Y<sub>2</sub>O<sub>3</sub> nanospheres for LED-phosphor applications: Synthesis and characterization," *Optics Express*, vol. 26, no. 26, pp. 34820-34829, 2018, doi: 10.1364/OE.26.034820.
- [14] A. Zhang *et al.*, "Tunable white light emission of a large area film-forming macromolecular complex with a high color rendering index," *Optical Materials Express*, vol. 8, no. 12, pp. 3635-3652, 2018, doi: 10.1364/OME.8.003635.
- [15] Y. Zhang, J. Wang, W. Zhang, S. Chen, and L. Chen, "LED-based visible light communication for color image and audio transmission utilizing orbital angular momentum superposition modes," *Optics Express*, vol. 26, no. 13, pp. 17300-17311, 2018, doi: 10.1364/OE.26.017300.
- [16] H. Ando and S. Ryu, "Simultaneous dual data stream transmission using RGB and phosphor-based white LEDs," *2018 Asia Communications and Photonics Conference (ACP)*, 2018, pp. 1-3, doi: 10.1109/ACP.2018.8596012.
- [17] S. Kashima *et al.*, "Wide field-of-view crossed dragone optical system using anamorphic aspherical surfaces," *Applied Optics*, vol. 57, no. 15, pp. 4171-4179, 2018, doi: 10.1364/AO.57.004171.
- [18] J. Chen, B. Fritz, G. Liang, X. Ding, U. Lemmer, and G. Gomard, "Microlens arrays with adjustable aspect ratio fabricated by electrowetting and their application to correlated color temperature tunable light-emitting diodes," *Optics Express*, vol. 27, no. 4, pp. A25-A38, 2019, doi: 10.1364/OE.27.000A25.
- [19] S. Jeon *et al.*, "Optical design of dental light using a remote phosphor light-emitting diode package for improving illumination uniformity," *Applied Optics*, vol. 57, no. 21, pp. 5998-6003, 2018, doi: 10.1364/AO.57.005998.
- [20] T. Hu *et al.*, "Demonstration of color display metasurfaces via immersion lithography on a 12-inch silicon wafer," *Optics Express*, vol. 26, no. 15, pp. 19548-19554, 2018, doi: 10.1364/OE.26.019548.
- [21] L. Li, Y. Zhou, F. Qin, Y. Zheng, and Z. Zhang, "On the Er<sup>3+</sup> NIR photoluminescence at 800 nm," *Optics Express*, vol. 28, no. 3, pp. 3995-4000, 2020, doi: 10.1364/OE.386792.
- [22] H. E. A. Mohamed, K. Hkiri, M. Khenfouch, S. Dhlamini, M. Henini, and M. Maaza, "Optical properties of biosynthesized nanoscaled Eu<sub>2</sub>O<sub>3</sub> for red luminescence applications" *Journal of the Optical Society of America A*, vol. 37, no. 11, pp. C73-C79, 2020, doi: 10.1364/JOSAA.396244.
- [23] A. K. Dubey, M. Gupta, V. Kumar, and D. S. Mehta, "Laser-line-driven phosphor-converted extended white light source with uniform illumination," *Applied Optics*, vol. 58, no. 9, pp. 2402-2407, 2019, doi: 10.1364/AO.58.002402.
- [24] J. Miao, M. Chen, Z. Chen, L. Zhang, S. Wei, and X. Yang, "Effect of Yb<sup>3+</sup> concentration on upconversion luminescence and optical thermometry sensitivity of La<sub>2</sub>MoO<sub>6</sub>: Yb<sup>3+</sup>, Er<sup>3+</sup> phosphors," *Applied Optics*, vol. 60, no. 6, pp. 1508-1514, 2021, doi: 10.1364/AO.412313.
- [25] S. S. Panda, H. S. Vyas, and R. S. Hegde, "Robust inverse design of all-dielectric metasurface transmission-mode color filters," *Optical Materials Express*, vol. 10, no. 12, pp. 3145-3159, 2020, doi: 10.1364/OME.409186.
- [26] D. Yan, S. Zhao, H. Wang, and Z. Zang, "Ultrapure and highly efficient green light emitting devices based on ligand-modified CsPbBr<sub>3</sub> quantum dots," *Photonics Research*, vol. 8, no. 7, pp. 1086-1092, 2020, doi: 10.1364/PRJ.391703.

## BIOGRAPHIES OF AUTHORS






**Huu Phuc Dang**    received a Physics Ph.D. degree from the University of Science, Ho Chi Minh City, in 2018. Currently, He is Research Institute of Applied Technology, Thu Dau Mot University, Binh Duong Province, Vietnam. His research interests include simulation LEDs material, renewable energy. He can be contacted at email: danghuuphuc@tdmu.edu.vn.



**Bui Van Hien**    is a lecturer at the Faculty of Mechanical - Electrical and Computer Engineering, School of Engineering and Technology, Van Lang University, Ho Chi Minh City, Viet Nam. His research interests are Optoelectronics (LED), Power transmission and Automation equipment. He can be contacted at email: hien.bv@vlu.edu.vn.



**Nguyen Le Thai**    received his BS in Electronic engineering from Danang University of Science and Technology, Vietnam, in 2003, MS in Electronic Engineering from Posts and Telecommunications Institute of Technology, Ho Chi Minh, Vietnam, in 2011 and PhD degree of Mechatronics Engineering from Kunming University of Science and Technology, China, in 2016. He is currently with the Nguyen Tat Thanh University, Ho Chi Minh City, Vietnam. His research interests include the renewable energy, optimisation techniques, robust adaptive control and signal processing. He can be contacted at email: nlthai@nttu.edu.vn.